ARL-TR-9274 ● AUG 2021

DEVCOM ARMY RESEARCH LABORATORY

Silver Ink Postprocessing Resistivity Optimization

by Thomas Parker and Jian Yu

NOTICES

Disclaimers

The findings in this report are not to be construed as an official Department of the Army position unless so designated by other authorized documents.

Citation of manufacturer's or trade names does not constitute an official endorsement or approval of the use thereof.

Destroy this report when it is no longer needed. Do not return it to the originator.

ARL-TR-9274 ● AUG 2021

Silver Ink Postprocessing Resistivity Optimization

Thomas Parker and Jian Yu
Weapons and Materials Research Directorate,
DEVCOM Army Research Laboratory

REPORT DOCUMENTATION PAGE

Form Approved
OMB No. 0704-0188

1. REPORT DATE *(DD-MM-YYYY)*	2. REPORT TYPE	3. DATES COVERED (From - To)
August 2021	Technical Report	1 February–9 August 2021

4. TITLE AND SUBTITLE
Silver Ink Postprocessing Resistivity Optimization

5a. CONTRACT NUMBER

5b. GRANT NUMBER

5c. PROGRAM ELEMENT NUMBER

6. AUTHOR(S)
Thomas Parker and Jian Yu

5d. PROJECT NUMBER

5e. TASK NUMBER

5f. WORK UNIT NUMBER

7. PERFORMING ORGANIZATION NAME(S) AND ADDRESS(ES)
DEVCOM Army Research Laboratory
ATTN: FCDD-RLW-ME
Aberdeen Proving Ground, MD 21005

8. PERFORMING ORGANIZATION REPORT NUMBER
ARL-TR-9274

9. SPONSORING/MONITORING AGENCY NAME(S) AND ADDRESS(ES)

10. SPONSOR/MONITOR'S ACRONYM(S)

11. SPONSOR/MONITOR'S REPORT NUMBER(S)

12. DISTRIBUTION/AVAILABILITY STATEMENT
Approved for public release: distribution unlimited.

13. SUPPLEMENTARY NOTES
ORCID ID: Thomas Parker, 0000-0002-6151-6815

14. ABSTRACT

The use of 3-D printing has gained a great deal of attention in multiple industries. The ability to create novel devices and structures in 3-D opens a range of applications that were previously not possible or prohibitively expensive. These 3-D printed materials very often do not have the same properties of their bulk counterparts. In this work, we examine the optimization of the postprocessing treatment of silver (Ag) printed ink. With the goal of minimizing the resistivity, in particular for high-frequency applications such as RF. Several approaches were investigated using temperature and/or local environment to control the sintering behavior of Ag ink. Both the atmosphere and energetics (plasma) of the atmosphere were examined in conjunction with temperature. The Ag inks were examined using X-ray diffraction, scanning electron microscopy, and a four-point probe to measure electrical resistivity. It was found that both temperature and gas environment had significant influences on the final ink resistivity. The use of multiple gasses lead to the best resistivity of 2.09E-8 ohm-m. Samples were annealed in air at 325 °C followed by a cool-down in a nitrogen (N_2) environment. It is postulated that the presence of air is necessary initially to decompose the organic ligands surrounding the Ag nanoparticles in the ink. The use of N_2 during the cool-down was to prevent the formation of silver oxide. The oxide is not present at 325 °C, as it decomposes at temperatures greater than 200 °. So by cooling in N_2, oxidation can be prevented and minimize the resistivity.

15. SUBJECT TERMS
3-D printing, resistivity, silver, Ag, annealing, grain size

16. SECURITY CLASSIFICATION OF:			17. LIMITATION OF ABSTRACT	18. NUMBER OF PAGES	19a. NAME OF RESPONSIBLE PERSON
a. REPORT	b. ABSTRACT	c. THIS PAGE			Thomas Parker
Unclassified	Unclassified	Unclassified	UU	17	19b. TELEPHONE NUMBER (Include area code) (410) 306-0870

Contents

List of Figures

List of Tables

1. Introduction

The use of 3-D printing to create novel combinations of materials or structures has garnered widespread interest in both industry and government. Activities such as prototyping can also be accomplished using 3-D printing, very often leading to significant reduction in both time and cost compared with traditional methods. However, one unfortunate aspect of 3-D printing is that very often the material properties of 3-D printed materials are not as good as their bulk or traditionally manufactured counterparts. For a given printing media there are two approaches to improve material properties. First, the parameters during printing can be optimized by changing things such as feed rates, temperature, and the amount of material put down during each step of the printing process. We are examining the second approach, namely, postprocessing. The ability to print high-quality metal is of great interest; specifically, when printing metal for electromagnetic applications such as circuitry and antennas. To optimize the performance of circuits and antennas, generally it is best to have a metal with as low a resistivity as possible. For bulk materials, silver (Ag) is the lowest resistivity metal at 1.59E-8 ohm-meter. Typical 3-D-printed Ag yields a resistivity in the hundreds of nano-ohm-meters. In this work, we explore various postprocess "annealing" steps to optimize the resistivity of 3-D printing Ag inks.

2. Methods, Assumptions, and Procedures

Ag ink was sourced from Navocentrix JS-A221AE ink with a specified Ag particle size smaller than 50 nm. A Keithley 2400 source measurement unit was run in four-wire mode with a resolution of 10 nV. Using a Jandel four-point probe head with a 60-g force and a 1-mm nominal probe spacing, measurements yielded a true probe spacing of 0.985 mm.

As films approach the resistivity of bulk Ag, the voltage drop for a typical electrical resistivity measurement at 100 mA approaches 10 nV. Driving more current results in sample heating and possible damage. While measuring voltage drops less than 10 nV requires specialized equipment, that will still be subject to significant levels of noise and measurement uncertainty. Increasing the current is not a solution, and attempting to measuring voltages below 10 nV is not plausible. To maximize the sensitivity of the electrical resistivity measurements, it is necessary to reduce the thickness of the Ag ink. To accomplish thin uniform layers, a process to spin-coat the Ag ink was developed. Silicon (Si) wafers were chosen as the substrate because they are very flat, nonconductive, and readily available. To achieve a uniform coating of the Ag ink, approximately 5 ml of Ag ink was manually spread with a

pipet over the surface of the 3-inch Si wafer. Immediately after, within 5–10 s the spin coater was started. It was found that a spin speed of 1000 rpm for 1 min resulted in uniform coating with a nominal film's thickness of approximately 500 nm. At a resistivity of 1.59E-8 ohm-m (bulk Ag), the four-point probe with the 0.985-mm probe spacing will yield a resistance of 5 milli-ohm at 100 mA corresponding to a voltage drop of 0.5 mV, well within the measurement range of our Keithley meter.

A Bruker D8 Discover equipped with a copper (Cu) X-ray tube and a 1-D position-sensitive X-ray detector were used in Bragg–Brentano geometry. For the in-situ heating measurements, an Anton-Paar DS1100 hot stage equipped with a graphite dome was used to heat the samples under different atmospheres while the sample X-ray diffraction (XRD) was measured. The in-situ heating scans were limited to the area around the Ag 111 peak (nominally 38.2° in 2-Theta). Each scan took 1 min to complete, and each temperature step took approximately 1 min to complete.

TOPAS Rietveld Software Ver. 5 was used to analyze the XRD data.

3. Results and Discussions

In Fig. 1, both cross-sectional and top-view scanning electron microscopy (SEM) images of the spin-coat Ag ink on a Si wafer are shown before and after annealing at 325 °C. In Fig. 1a, the cross-section of an unannealed spin-coat Ag ink is shown. Smooth Si substrate can be seen in the bottom of the image and the spin-coated Ag film above. The particles in the Ag film are observed to be in the 50-nm size range. The total film thickness is 526 nm. In Fig. 1b, the cross-sectional SEM of the sample annealed at 325° C in air for 10 min then cooled in nitrogen (N_2). The small Ag particles can no longer observed due to sintering, and the film thickness is 426 nm. In Fig. 1c, the top view of the unannealed Ag ink is shown, and the Ag particles are clearly observed as well as circular voids (dark circles) formed as the solvent evaporated from the ink during spin coating. In Fig. 1d, the top view of the annealed film is shown. The small particles have been replaced with large grains on the order of several hundred nanometers. The lines or striping within the grains are likely due to electron channeling contrast. The differences in channeling are likely due to twinning within the individual grains. The small circular voids seen in Fig. 1c have been replaced by larger, more dispersed voids indicating significant atomic mobility during the annealing process.

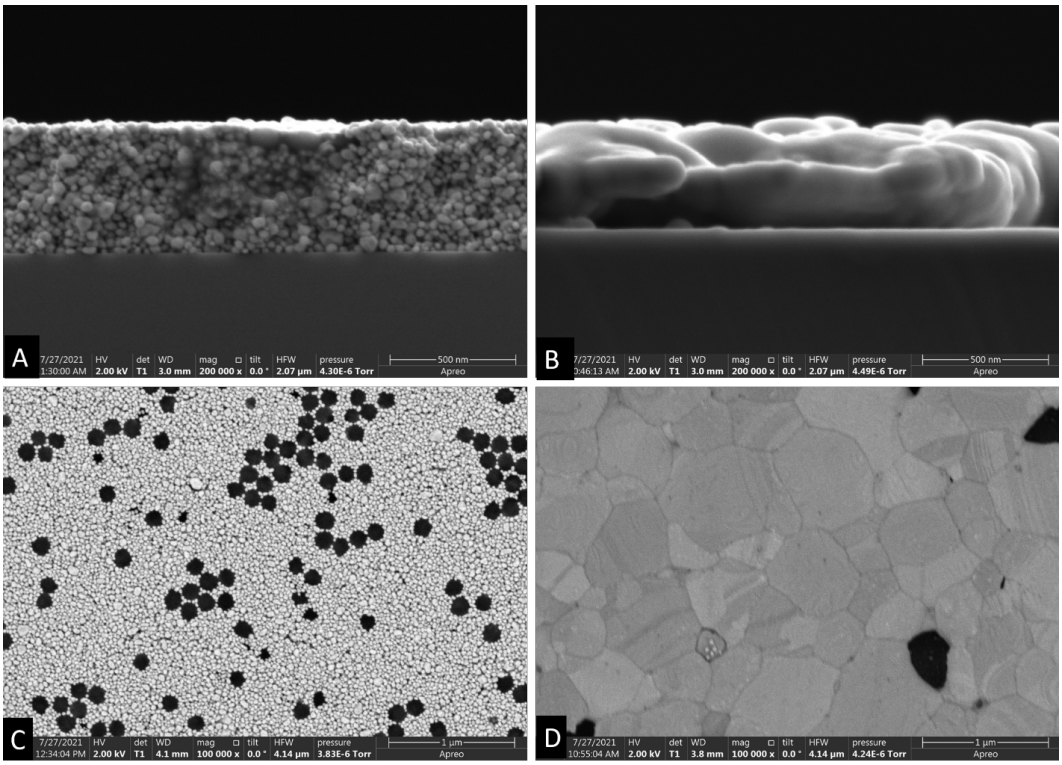

Fig. 1 A) Ag ink spin-coat unannealed SEM cross-section, B) Ag ink spin-coat 325 °C annealed N_2 cool-down SEM cross-section, C) Ag ink spin-coat unannealed SEM top view, and D) Ag ink spin-coat 325 °C annealed N_2 cool-down SEM top view

In Fig. 2, the XRD scans of the Ag 111 peaks versus temperature are shown. Along the y-axis is the square root of the counts, and along the x-axis is the 2-Theta value. Starting from the front, the back shows the room temperature Ag 111 peak. The temperature of the individual scans is sequentially increased, with the temperature increasing from front to the back. Starting at room temperature 25 °C (black curve), the temperature was incremented in steps of 25 °C. The green curve furthest back corresponds to the final temperature of 400 °C. It can be observed that the peak at 25 °C is very broad without any evidence of the separation between the k α1 and k α2 Cu X-ray peaks. As the temperature increases, the peaks sharpen and begin to show the k-alpha doublet, indicating increasing crystallite size. At 400 °C, the peak is very sharp with a well-defined k-alpha doublet.

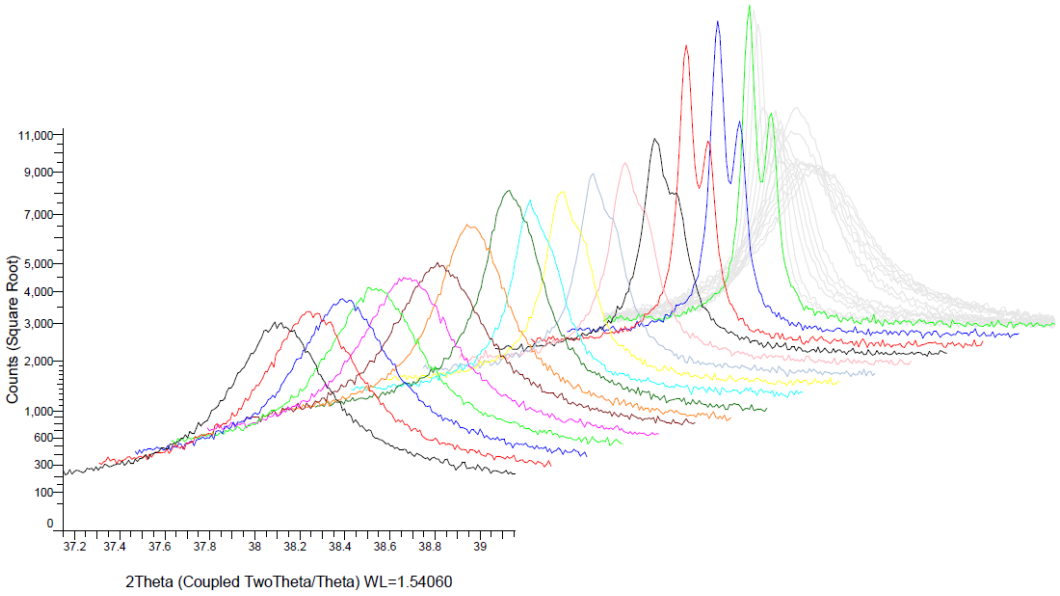

Fig. 2 XRD of Ag ink (111) planes on Si wafer vs. temperature

Figure 3 shows the crystallite size as derived from the XRD scans shown in Fig. 2. The TOPAS software package was used to model and fit the X-ray peaks using the Reitveld method to determine the crystallite size. The log of the crystallite size is shown in the y-axis as a function of the sample temperature in degrees Celsius along the x-axis. The as-deposited (spin-coat) film shows a grain size of approximately 30 nm. This is in agreement with the SEM images in Fig. 1a and 1c, and agrees as well as with the manufacturer's specification of particles less than 50 nm. This grain size was found to be stable until the sample reached a temperature of 150 °C, after which the grain size quickly increased in size. This grain growth then stabilized at 200 °C at a value of approximately 100 nm. The grain size is stable at this size until reaching a temperature of 325 °C, after which the grain size begins to quickly continue to increase to the few-micron range until reaching a temperature of 400 °C.

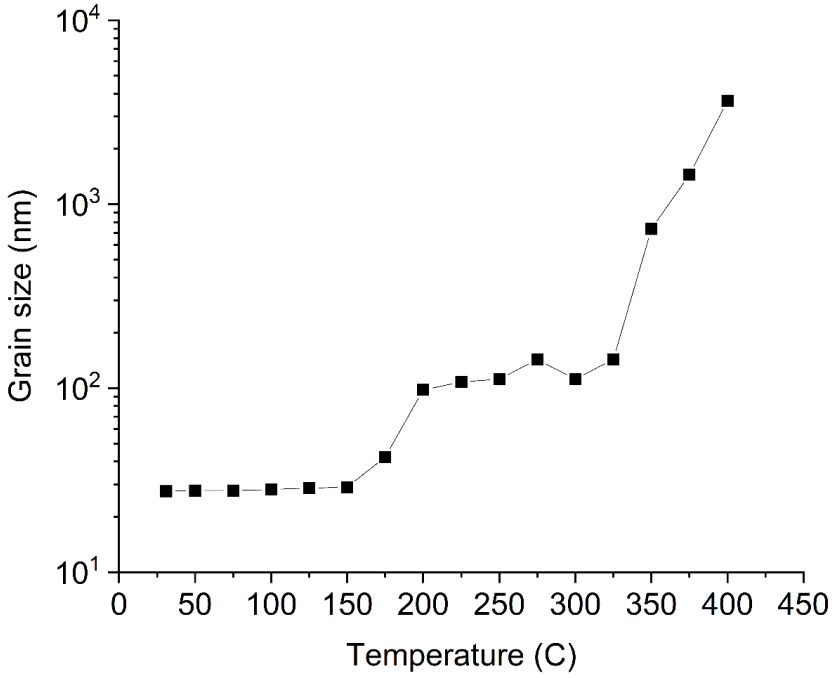

Fig. 3 Grain size of Ag ink using the width of the Ag (111) diffraction peak vs. temperature

A four-point probe was used to measure the electrical resistance in ohms of each sample.

Equation 1 is the four-point probe resistivity correction for sample thickness and lateral size.

$$\rho = \frac{\pi}{\ln(2)}\frac{V}{I}tf_1f_2 = 4.53 * R * t * \frac{\ln(2)}{\ln\left[\frac{\sinh(\frac{t}{s})}{\sinh(\frac{t}{2s})}\right]} * \frac{1}{1+\frac{2}{\sqrt{1+(\frac{d}{s})^2}}-\frac{1}{\sqrt{1+(\frac{d}{2s})^2}}} \quad (1)$$

The resistance value along with the thickness measured using cross-sectional SEM is used to derive the resistivity of the sample using Eq. 1,[1] where ρ is the resistivity, V is the applied voltage, I is the resultant current, and t is the thickness of the sample. The correction factors for finite sample thickness (f_1) and finite sample lateral dimensions (f_2), where s is the probe spacing and d is the sample's lateral size assuming a square. For all of our samples, the lateral dimension had little effect on the derived resistivity, as our typical sample size is 40 mm and the probe spacing is approximately 1 mm, resulting in the f_2 term being near unity. However, the f_1 term has a strong effect because our thickness t is much smaller than the spacing. In Table 1, the measured thickness and resistance for each sample is shown. The standard deviation of the resistance measurement was typically on the order of 1%. The resistivity calculated using Eq. 1 is shown in the finale column. All treated samples were either annealed or plasma treated for 10 min. The heated samples

were annealed in air and then cooled in air (180 °C), annealed in air then cooled in N_2 (air 230 °C N_2), or annealed and cooled in N_2 (N_2 180 °C).

Table 1 Thickness and resistance

Sample description	Thickness (nm)	Mean resistance (ohm)	Resistance standard deviation	Calculated resistivity (ohm-m)
Unannealed	589	1.664E7	2.54E5	4.44E4
N_2 180 °C	775	1.86E5	1.16E4	1.53E0
O_2 plasma	538	1.88E3	6.78E1	4.59E-3
N_2 180 °C air	576	4.49E-1	2.24E-1	8.84E-5
Argon plasma	705	3.03E-1	5.59E-3	9.68E-7
Air 180 °C	482	2.65E-2	1.2E-3	5.79E-7
Air 230 °C N_2	54,000	4E-4	1E-4	9.78E-8
Air 325 °C	485	1.20E-2	9.49E-4	2.63E-8
Air 325 °C N_2	426	1.08E-2	7.03E-4	2.09E-8

In Fig. 4, the resistivity values from Table 1 are plotted from largest (unannealed) to least (Bulk Ag) in a logarithmic scale in the y-axes versus the samples processing history. As can be seen, the annealed samples achieved the lowest resistivity, where the temperature of the anneal strongly correlated with decreasing resistivity. The samples annealed at 325 °C and cooled in N_2 had the lowest resistivity out of any sample, while the sample annealed at 325 °C and cooled in air had the next lowest.

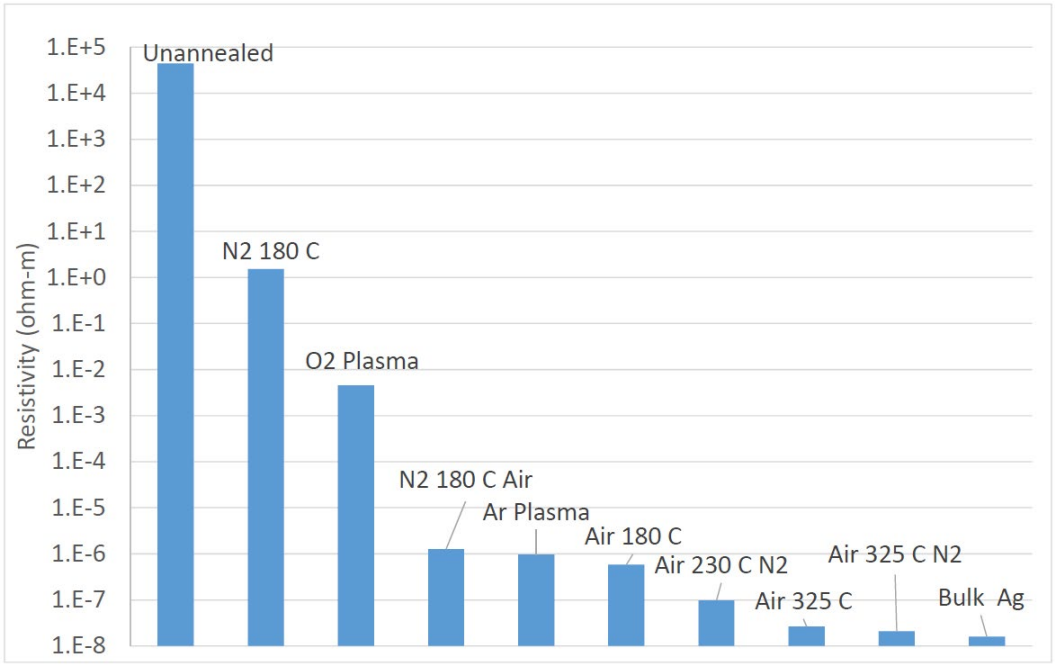

Fig. 4 Resistivity values as a function of processing from Table 1

In Fig. 5, the resistivity and inverse grain size in nanometers are plotted for several samples. The resistivity is plotted in a bar chart with the values in left y-axis in a logarithmical scale. The inverse grain size is plotted as a scatter plot indicated by black squares, with the values in the right y-axis logarithmically. As can be seen, as the inverse grain-size value decreases, or conversely as the grain size increases, the resistivity decreases. This increasing grain size and decreased resistivity indicate that the limiting factor in the electric conduction is the intragranular electron transmission. The manufacturer of our Ag ink does not disclose what ligand is used to stabilize the Ag nanoparticles. However, organic ligands in general will decompose in steps usually initiating in the 100–200 °C range,[3] followed by subsequent decomposition steps at higher temperatures, permitting grain growth and a corresponding reduction in resistivity.

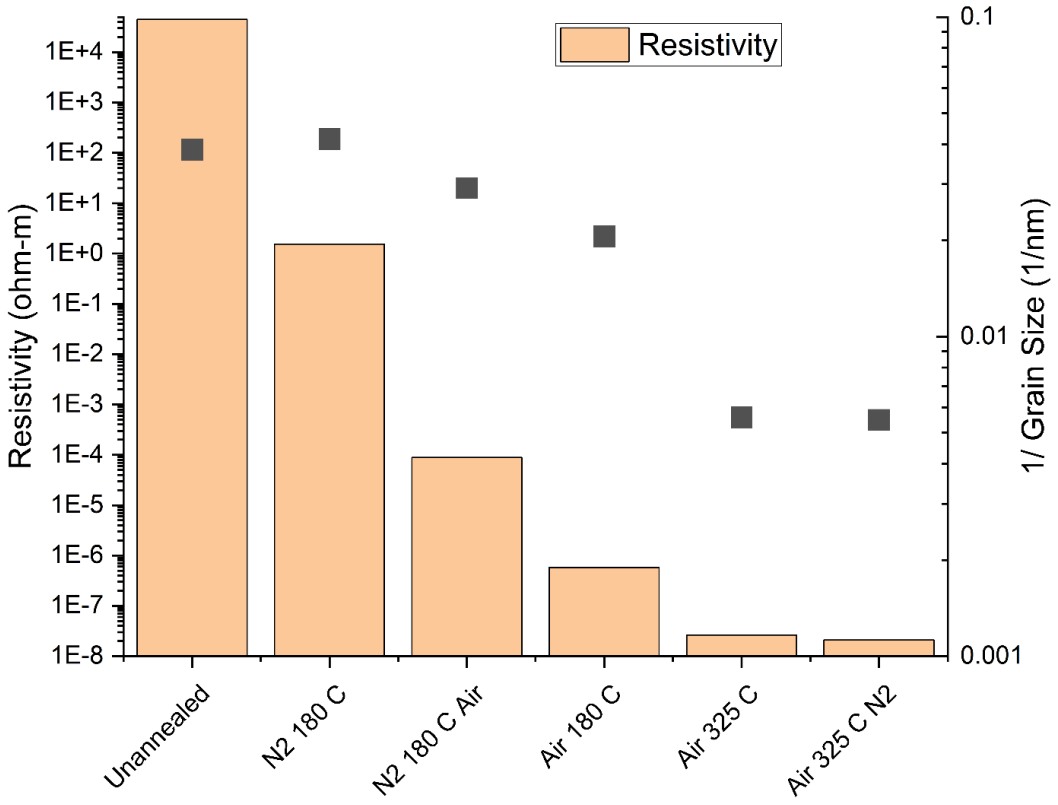

Fig. 5 Resistivity plotted against the inverse grain size for several samples

4. Conclusion

We have shown that moderate increase in temperature to 230 °C, 50 °C above the manufacturer's recommended temperature (180 °C), in conjunction with sample cooling under an inert atmosphere (N_2), leads to almost a 1 order of magnitude decrease in the resistivity.

For extremely temperature sensitive substrates that cannot sustain 180 °C, argon plasma was found to achieve a resistivity value of 9.68E-7 ohm-m, roughly double that achieved using the manufacturer's recommended 180 °C in air. However, this may be sufficient for some applications. A typical substrate temperature reached during plasma processing is 50–80 °C.

Samples annealed at 325 °C in air followed by an N_2 cool-down achieved a resistivity value of 2.09E-8 ohm-m, which is 20% lower than annealing at 325 °C and cooling in air. We found that during the initial annealing, air was necessary to presumably help oxidize and decompose the protective ligand. Once the ligand was decomposed, cooling under the inert N_2 gas prevented oxidation of the Ag, thus maintaining a low resistivity.

5. References

1. Smits FM. Measurement of sheet resistivities with the four-point probe. The Bell System Technical Journal. 1958 May;37(3):711–718. doi: 10.1002/j.1538-7305.1958.tb03883.x.

2. Chaudhary RG, Ali P, Gandhare NV, Tanna JA, Juneja HD. Thermal decomposition kinetics of some transition metal coordination polymers of fumaroyl bis (paramethoxyphenylcarbamide) using DTG/DTA techniques. Arabian Journal of Chemistry. 2019;12(7):1070–1082. https://doi.org/10.1016/j.arabjc.2016.03.008.

List of Symbols, Abbreviations, and Acronyms

1-D	one-dimensional
3-D	three-dimensional
Ag	silver
Cu	copper
f_1	finite sample thickness
f_2	finite sample lateral dimensions
SEM	scanning electron microscopy
Si	silicon
XRD	X-ray diffraction

1 (PDF)	DEFENSE TECHNICAL INFORMATION CTR DTIC OCA
1 (PDF)	DEVCOM ARL FCDD RLD DCI TECH LIB
18 (PDF)	DEVCOM ARL FCDD RLD S SILTON FCDD RLW J ZABINSKI A RAWLETT S KARNA J NEWILL S SCHOENFELD FCDD RLW B J LASALVIA FCDD RLW M E CHIN FCDD RLW MC JF SNYDER FCDD RLW MD J LA SCALA J YU A BUJANDA FCDD RLW ME TC PARKER N KU A DIGIOVANNI V BLAIR W SHOULDERS L VARGAS-GONZALEZ